Sex- and Age-Dependent Neuroimmune Dysregulation and Early Neurodegenerative Signatures Following SARS-CoV-2 Infection in Golden Syrian Hamsters

Narendra Kumar[1#], Arpan Acharya[1#], Rajesh Das[2], Urvinder Kaur Sardarni[1], Olasunkanmi Israel Tayo[1], Swathi Priyanka Murakonda[1], Debapriya Sutar[1], Amouda Venkatesan[2], Dinakara Rao Ampasala[2], Samuel M. Cohen[3], Mystera M. Samuelson[4], Balasrinivasa R. Sajja[5], Ulf Dettmer[6], Nagendran Ramalingam[6], Hitendra S. Chand[7], Siddappa N. Byrareddy[1*].

Affiliations:

[1]Department of Pharmacology and Experimental Neuroscience, University of Nebraska Medical Center, Omaha, NE, USA.

[2]Department of Bioinformatics, School of Life Sciences, Pondicherry University, Puducherry 605014, India.

[3]Sylvia Havlik Centennial Professor of Oncology, Department of Pathology, Microbiology, and Immunology and the Buffett Cancer Center, University of Nebraska Medical Center, Omaha, NE, USA.

[4]Department of Environmental, Agricultural, and Occupational Health, The University of Nebraska Medical Center, Omaha, Nebraska, USA

[5]Department of Radiology, University of Nebraska Medical Center, Omaha, NE, USA

[6]Ann Romney Center for Neurologic Diseases, Brigham and Women's Hospital and Harvard Medical School, Boston, MA 02115, USA

[7]Department of Cellular and Molecular Medicine, Herbert Wertheim College of Medicine, Florida International University, Miami, Florida, USA

[*]Correspondence: sid.byrareddy@unmc.edu

[#] equal contribution

Keywords: Long-COVID, PASC, GSH, Neuroinflammation, Animal model, Sex-differences

Supplementary materials

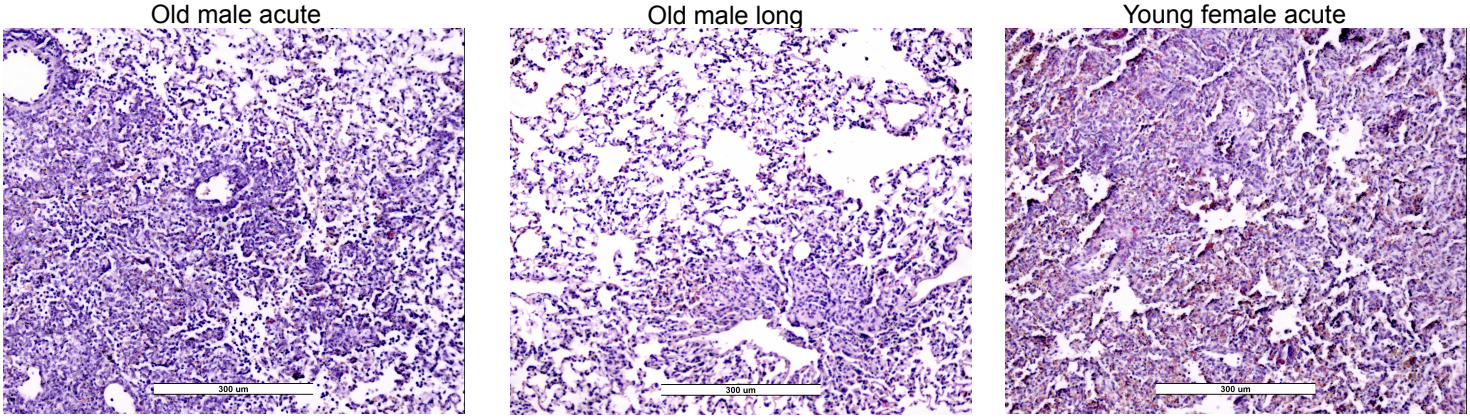

Supplementary figure 1: Hematoxylin and Eosin (H&E) stained lung sections showing evidence of aplasia in old male during acute and long COVID) and a young female hamster (during acute COVID).

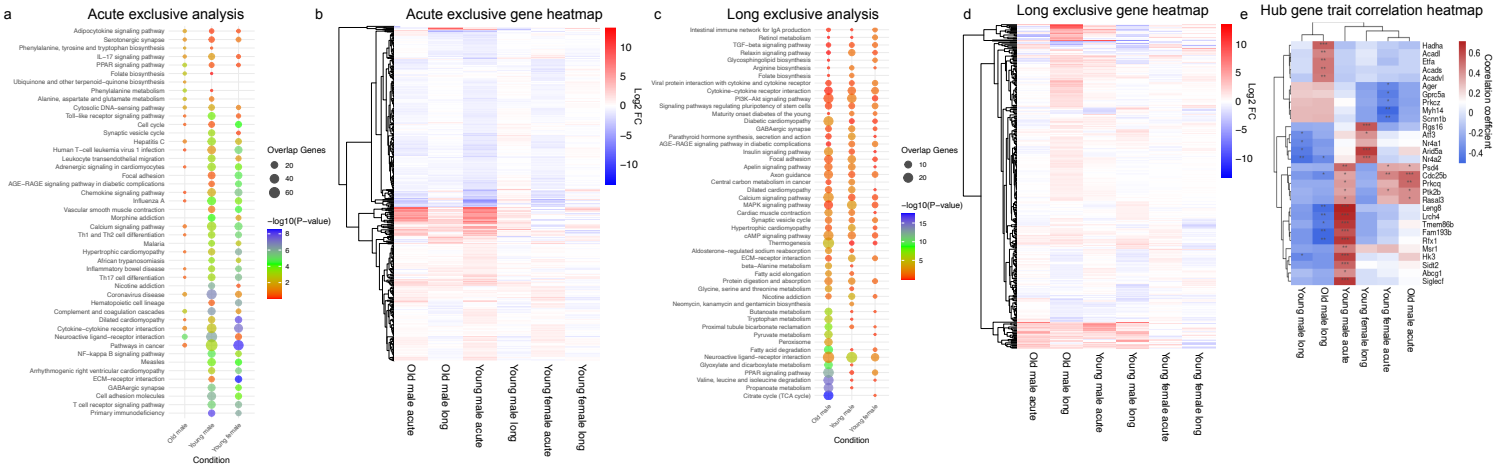

Supplementary figure 2: Signaling and inflammation-related pathways identified in lung transcriptomic analysis during acute and long-term infection. (a) Combined pathway analysis bubble plot depicting significantly enriched pathways across different groups (old male, young male, young female) during acute infection. Bubble size indicates the number of overlapping genes, while color intensity corresponds to the $-\log_{10}$(P-value). (b) Heatmap of gene expression showing $\log_2$ fold changes of differentially expressed genes (DEGs) associated with the identified pathways across different groups during acute infection in the lung, with their expression status compared across conditions. (c) Combined pathway analysis bubble plot depicting significantly enriched pathways across different groups (old male, young male, young female) during Long COVID. Bubble size indicates the number of overlapping genes, while color intensity corresponds to the $-\log_{10}$(P-value). (d) Heatmap of gene expression showing $\log_2$ fold changes of differentially expressed genes (DEGs) associated with the identified pathways across different groups during Long COVID in the lung, with their expression status compared across conditions. (e) Heatmap of top module hub genes (top 5 per module) showing gene–trait correlations with significance (*$p \le 0.05$, **$p \le 0.01$, ***$p \le 0.001$)

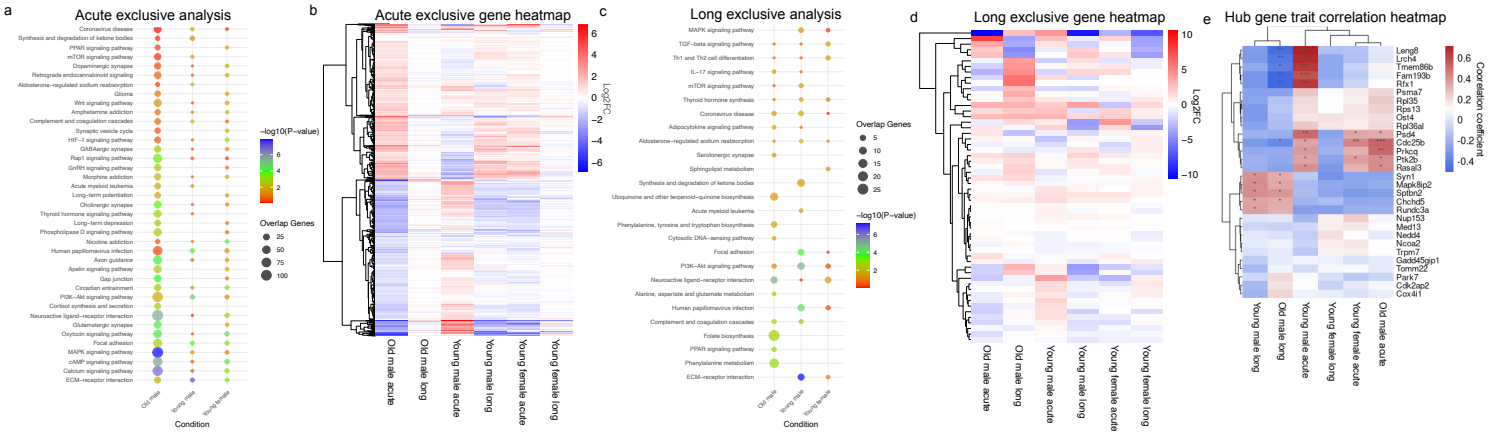

Supplementary figure 3: Signaling and synaptic system related pathways identified in Brain transcriptomic analysis during acute and long-term infection. (a) Combined pathway analysis bubble plot depicting significantly enriched pathways across different groups (old male, young male, young female) during acute infection. Bubble size indicates the number of overlapping genes, while color intensity corresponds to the $-\log_{10}$(P-value). (b) Heatmap of gene expression showing $\log_2$ fold changes of differentially expressed genes (DEGs) associated with the identified pathways across different groups during acute infection in the lung, with their expression status compared across conditions. (c) Combined pathway analysis bubble plot depicting significantly enriched pathways across different groups (old male, young male, young female) during Long COVID. Bubble size indicates the number of overlapping genes, while color intensity corresponds to the $-\log_{10}$(P-value). (d) Heatmap of gene expression showing $\log_2$ fold changes of differentially expressed genes (DEGs) associated with the identified pathways across different groups during Long COVID in the lung, with their expression status compared across conditions. (e) Heatmap of top module hub genes (top 5 per module) showing gene–trait correlations with significance (*p ≤ 0.05, **p ≤ 0.01, ***p ≤ 0.001)

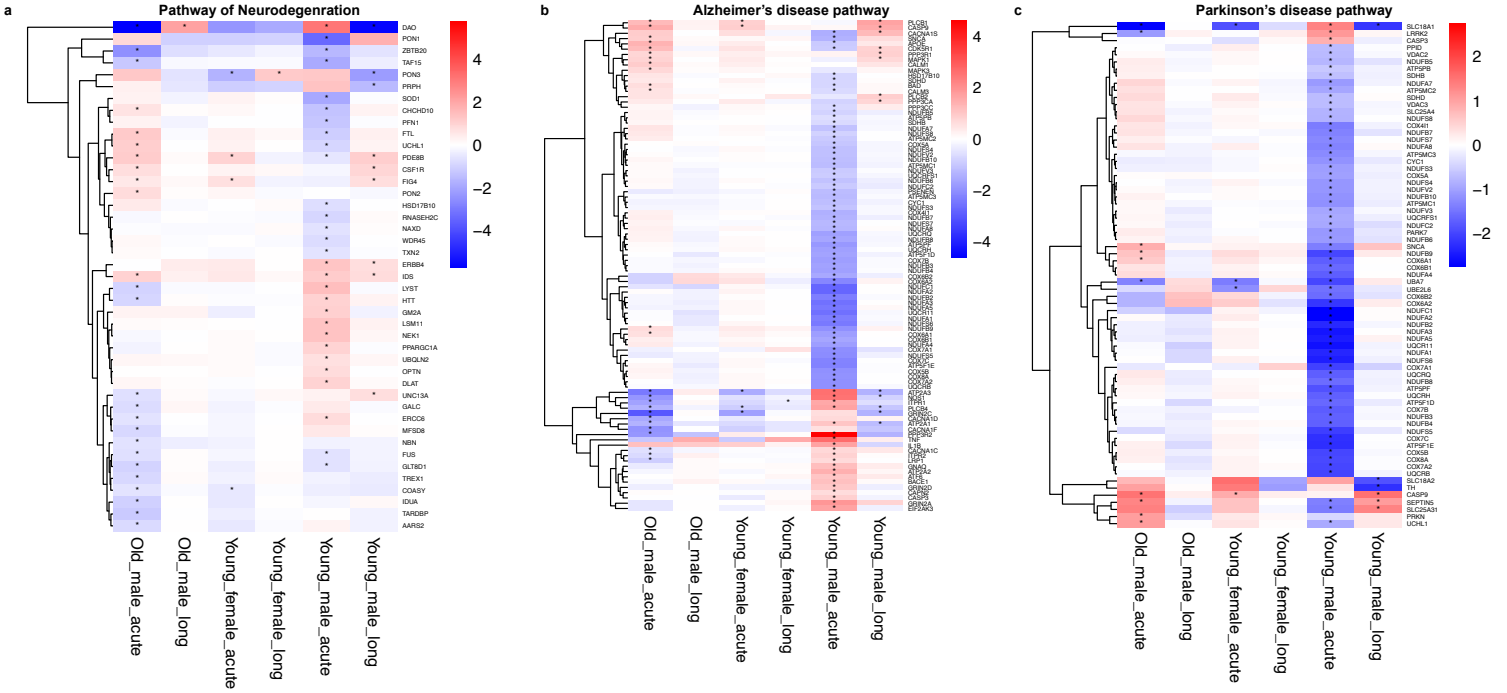

Supplementary figure 4: SARS-CoV-2 infection affects the expression of genes related to neurodegeneration, Alzheimer's and Parkinson's disease pathway with Young male showing highest significantly altered gene during Long-COVID. (a) Heatmap showing the differentially expressed genes at 4 and 30 dpi according to the selected KEGG pathway "Pathway of Neurodegeneration" (b),"Alzheimer's disease pathway " (c) "Parkinson's disease pathway" calculated in comparison with mock-infected hamsters. Color gradient represents the transcription log2 fold change comparing infected and mock-infected derived from EdgeR differential expression analysis with TMM normalization. Statistical significance in heatmaps is indicated by asterisks based on raw p-values: * ($p < 0.05$), ** ($p < 0.001$), *** ($p < 0.0001$).

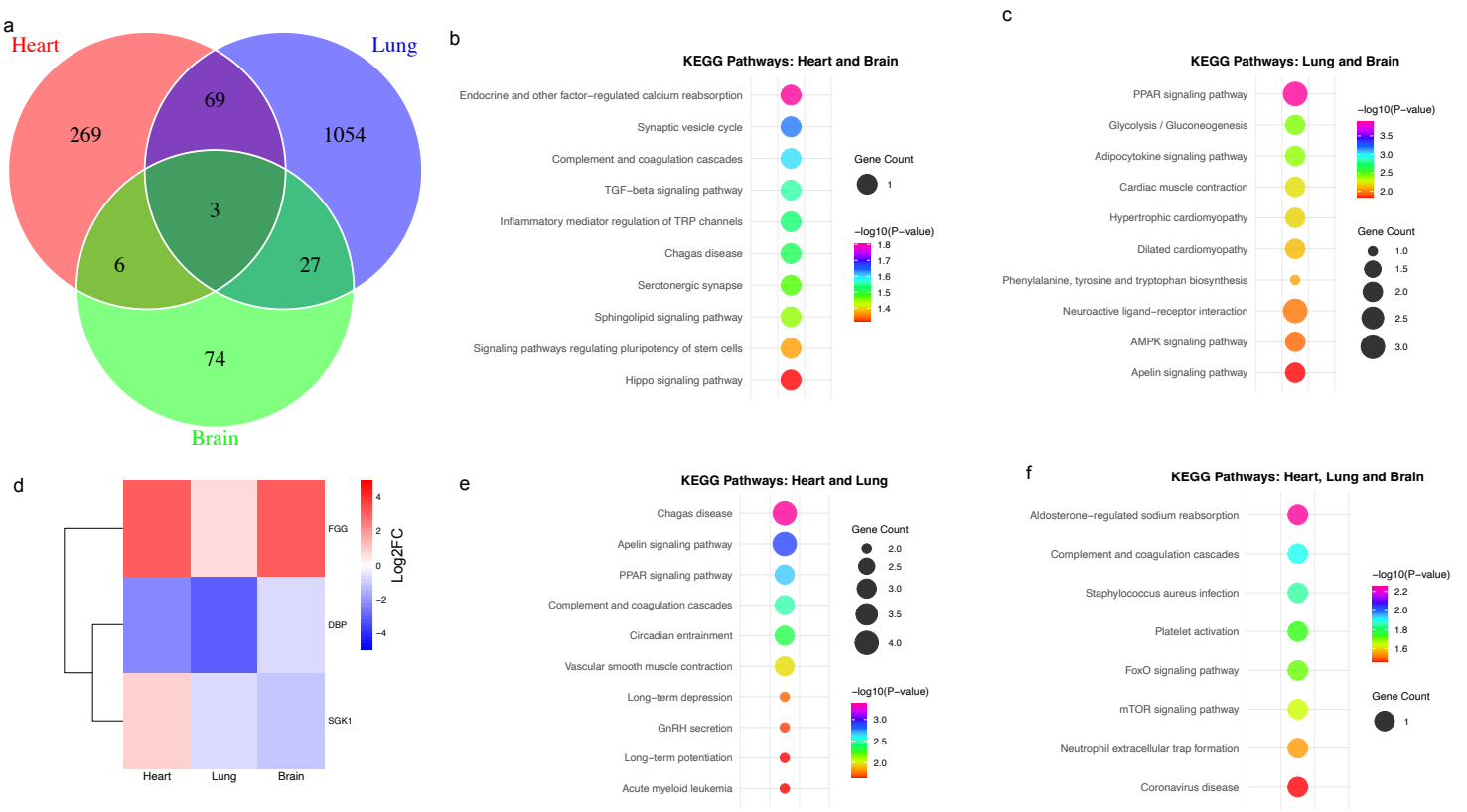

Supplementary figure 5: Comparative analysis of transcriptomic data in Long-COVID across different organ systems in Old male group. (a) Venn diagram showing overlap of differentially expressed genes between Heart, Lung, and Brain tissues during Long-COVID. (b,c,e,f) KEGG pathway enrichment analysis showing top 10 significantly altered common pathways between different organ systems. Bubble size indicates the number of overlapping genes, while color intensity corresponds to the $-\log_{10}$(P-value). (d) Heatmap displaying organ-specific gene expression patterns in common DEGs identified across all the three organs, with red indicating upregulation and blue indicating downregulation. Rows represent individual genes and columns represent the three organ systems (Heart, Lung,

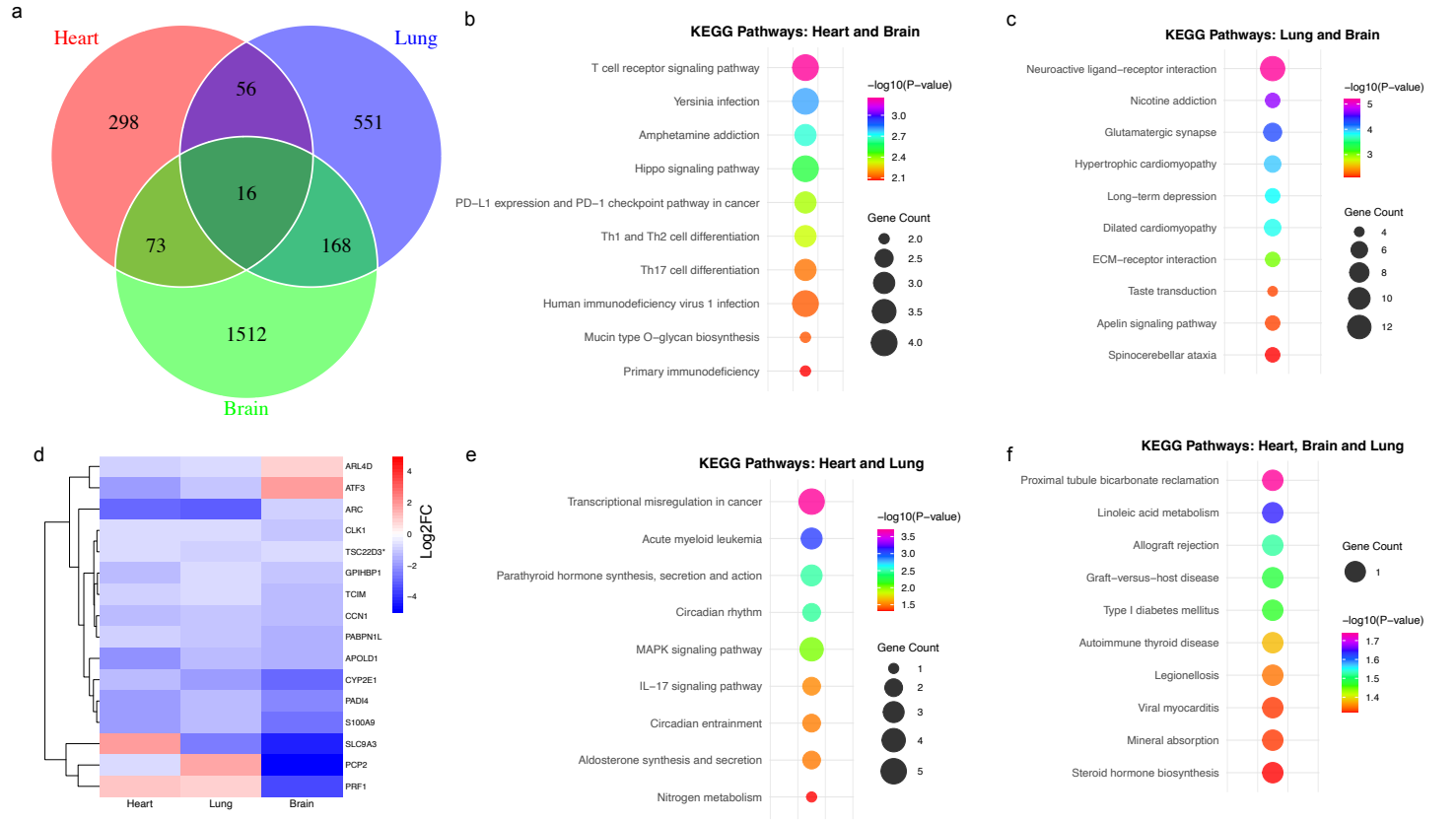

Supplementary figure 6: Comparative analysis of transcriptomic data in Long-COVID across different organ systems in Young male group. (a) Venn diagram showing overlap of differentially expressed genes between Heart, Lung, and Brain tissues during Long-COVID. (b,c,e,f) KEGG pathway enrichment analysis showing top 10 significantly altered common biological pathways between different organ systems. Bubble size indicates the number of overlapping genes, while color intensity corresponds to the $-\log_{10}$(P-value). (d) Heatmap displaying organ-specific gene expression patterns in common DEGs identified across all the three organs, with red indicating upregulation and blue indicating downregulation. Rows represent individual genes and columns represent the three organ systems (Heart, Lung, Brain).

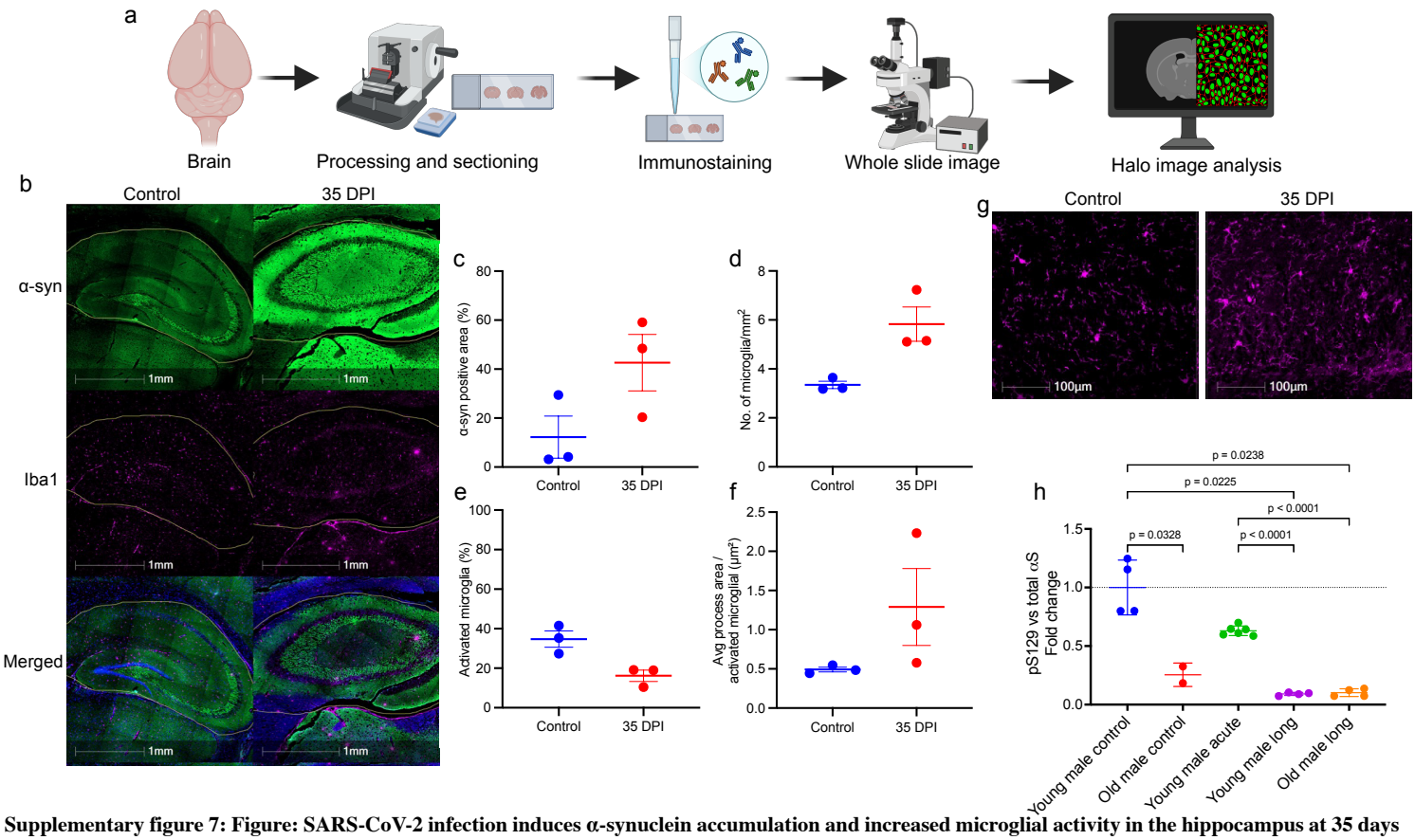

Supplementary figure 7: Figure: SARS-CoV-2 infection induces α-synuclein accumulation and increased microglial activity in the hippocampus at 35 days post-infection (DPI). (a) Schematic workflow illustrating brain tissue processing for immunostaining and quantification of protein expression changes. (b) Representative images of the hippocampus showing α-synuclein (green), Iba1-labeled microglia (magenta), and merged images with DAPI (blue) in control and 35 DPI animals. (c) Quantification of α-synuclein (α-syn) positive area in the hippocampus, showing increased accumulation at 35 DPI. (d) Quantification of microglial number per mm², showing an increase in microglial population at 35 DPI. (e) Percentage of activated microglia among total microglia showing decreased percentage of activated microglia. (f) Average process area per activated microglia showing increase in average process area at 35 DPI. (g) Representative high-magnification images of microglia in control and infected hippocampi stained with Iba1 (magenta). Data represent mean ± SEM. (h) Fold change in phospho-S129 α-synuclein (pS129) versus total α-synuclein across different groups, showing significant increases in infected young and old animals in both acute and long phases compared to controls. Statistical comparisons were conducted using Welch's ANOVA followed by Dunnett's T3 multiple comparisons test to account for heterogeneity in variances and unequal sample sizes.

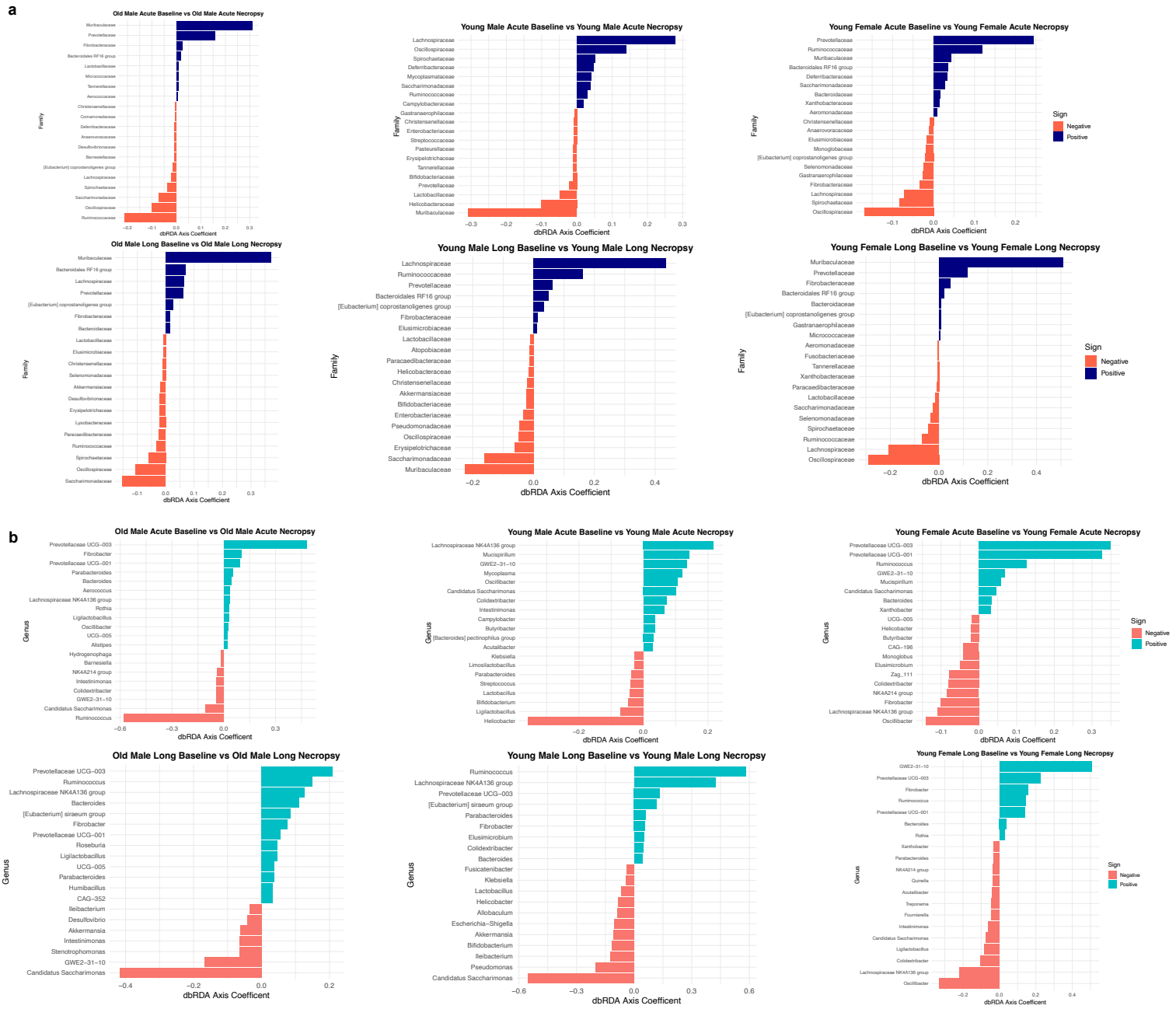

Supplementary figure 8: Bar plot depicting the top 20 group-specific microbial (a) families and (b) genera across different groups. Differences were assessed using Distance-based Redundancy Analysis (dbRDA) and Canonical Analysis of Principal Coordinates (CAP) at both the family and genus levels.

Supplementary Table 1: RNA sequencing details of Lung and Brian samples

S.No	Group	ID	Lung	Brain
1	Old Male Control	6	Yes	No
2	Old Male Control	7	Yes	Yes
3	Old Male Control	8	Yes	Yes
4	Old Male Control	16	Yes	Yes
5	Old Male Control	17	Yes	Yes
6	Old Male Acute	458	Yes	Yes
7	Old Male Acute	460	Yes	Yes
8	Old Male Acute	462	Yes	Yes
9	Old Male Acute	463	Yes	Yes
10	Old Male Long	448	Yes	Yes
11	Old Male Long	449	Yes	Yes
12	Old Male Long	450	Yes	Yes
13	Old Male Long	451	Yes	Yes
14	Young Male Control	1	Yes	Yes
15	Young Male Control	2	Yes	Yes
16	Young Male Control	3	Yes	Yes
17	Young Male Control	4	Yes	Yes
18	Young Male Acute	131	No	Yes
19	Young Male Acute	133	Yes	Yes
20	Young Male Acute	134	Yes	Yes
21	Young Male Acute	135	Yes	Yes
22	Young Male Long	442	Yes	Yes
23	Young Male Long	443	Yes	Yes
24	Young Male Long	444	Yes	Yes
25	Young Male Long	445	Yes	Yes
26	Young Female Control	11	Yes	Yes
27	Young Female Control	12	Yes	Yes
28	Young Female Control	13	Yes	Yes
29	Young Female Control	14	Yes	Yes
30	Young Female Acute	452	Yes	Yes
31	Young Female Acute	454	Yes	Yes
32	Young Female Acute	455	Yes	Yes
33	Young Female Acute	457	Yes	Yes
34	Young Female Long	495	Yes	Yes
35	Young Female Long	497	Yes	Yes
36	Young Female Long	498	Yes	Yes
37	Young Female Long	499	Yes	Yes

Supplementary Table 2: RNA sequencing details of Heart samples

S. No	Group	Sample id	Heart
1	Old Male Control	5	Yes
2	Old Male Control	6	Yes
3	Old Male Control	7	Yes
4	Old Male Control	8	Yes
5	Old Male Control	9	Yes
6	Old Male Control	16	Yes
7	Old Male Long	489	Yes
8	Old Male Long	490	Yes
9	Old Male Long	491	Yes
10	Old Male Long	492	Yes
11	Old Male Long	493	Yes
12	Young Male Control	1	Yes
13	Young Male Control	2	Yes
14	Young Male Control	3	Yes
15	Young Male Control	4	Yes
16	Young Male Control	19	Yes
17	Young Male Control	20	Yes
18	Young Male Long	440	Yes
19	Young Male Long	441	Yes
20	Young Male Long	442	Yes
21	Young Male Long	443	Yes
22	Young Male Long	444	Yes
23	Young Male Long	445	Yes